Relativistic jets from stellar black holes

Gallo, E.

Publication date
2005

CHAPTER 2

A UNIVERSAL RADIO:X-RAY CORRELATION IN LOW/HARD STATE BLACK HOLE BINARIES

Elena Gallo, Rob Fender & Guy Pooley
Monthly Notices of The Royal Astronomical Society 344, 60-72 (2003)

Several independent lines of evidence now point to a connection between the physical processes that govern radio (*i.e.* jet) and X-ray emission from accreting X-ray binaries. We present a comprehensive study of (quasi-)simultaneous radio:X-ray observations of stellar black hole binaries during the spectrally hard X-ray state, finding evidence for a strong correlation between these two bands over more than three orders of magnitude in X-ray luminosity. The correlation extends from the quiescent regime up to close to the soft state transition, where radio emission starts to decline, sometimes below detectable levels, probably corresponding to the physical disappearance of the jet. The X-ray transient V 404 Cygni is found to display the same functional relationship already reported for GX 339–4 between radio and X-ray flux, namely $S_{\rm radio} \propto S_{\rm X}^{+0.7}$. In fact the data for all low/hard state black holes is consistent with a universal relation between the radio and X-ray luminosity of the form $L_{\rm radio} \propto L_{\rm X}^{+0.7}$. Under the hypothesis of common physics driving the disc–jet coupling in different sources, the observed spread to the best-fit relation can be interpreted in terms of a distribution in Doppler factors and hence used to constrain the bulk Lorentz factors of both the radio and X-ray emitting regions. Monte Carlo simulations show that, assuming little or no X-ray beaming, the measured scatter in radio power is consistent with Lorentz factors $\lesssim 2$ for the outflows in the low/hard state, significantly less relativistic than the jets associated with X-ray transients. When combined radio and X-ray beaming is considered, the range of possible jet bulk velocities significantly broadens, allowing highly relativistic outflows, but implying therefore severe X-ray selection effects. If the radio luminosity scales as the total jet power raised to $x > 0.7$, then there exists an X-ray luminosity below

which most of the accretion power will be channelled into the jet, rather than in the X-rays. For $x = 1.4$, as in several optically thick jet models, the power output of 'quiescent' black holes may be jet-dominated below $L_{\rm X} \simeq 4 \times 10^{-5}\ L_{\rm Edd}$.

2.1 Introduction

There is strong observational evidence for the fact that powerful radio-emitting outflows form a key part of the accretion behaviour in some states of X-ray binary systems. Due to its high brightness temperature, 'nonthermal' spectrum and, in some cases, high degree of polarisation, radio emission from black hole binaries is believed to originate in synchrotron radiation from relativistic electrons ejected by the system with large bulk velocities (Hjellming & Han 1995; Mirabel & Rodríguez 1999; Fender, 2000, 2001a,b,c).

Black hole binary systems are traditionally classified by their X-ray features (see Nowak 1995; Poutanen 1998; Done 2001; Merloni 2002 for recent reviews), namely: a) the relative strength of a soft 'black body' component around 1 keV, b) the spectral hardness at higher energies c) X-ray luminosity and d) timing properties. Different radio properties are associated with several 'X-ray states', according to the following broad scheme. The *low/hard state* is dominated by a power-law spectrum, with a relatively low luminosity and an exponential cut-off above about 100 keV and little or no evidence for a soft, thermal component. It is associated with a steady, self-absorbed outflow that emits synchrotron radiation in the radio (and probably infrared) spectrum. The *quiescent/off state*, characterised by an extremely low X-ray flux, may simply be interpreted as the hard state 'turned down' to lower accretion rates and radiative efficiency. X-ray spectra from *high/soft state* Black Hole Candidates (BHCs) are instead dominated by thermal radiation, while the core radio emission drops below detectable levels, probably corresponding to the physical suppression of the jet. In the *very high state* both the thermal and the power law components contribute substantially to the spectral energy distribution. At a lower luminosity level an *intermediate state* is also observed, with properties similar to those of the very high state. For both the very high and the intermediate state the connection with radio behaviour is not yet clearly established. Corbel et al. (2001) show that the radio emission from XTE 1550–564 in the intermediate state was suppressed by a factor > 50 with respect to the hard state, while Homan et al. (2001) claim that intermediate and very high states can actually occur at a wide range of luminosities.

Transitions between states are often associated with multiple ejections of synchrotron emitting material, possibly with high bulk Lorentz factors (Hjellming

& Han 1995; Kuulkers et al. 1999; Fender & Kuulkers 2001).
As already mentioned, BHCs in the low/hard state, like Cygnus X–1 and GX 339–4, are characterised by a flat or slightly inverted radio spectrum ($\alpha = \Delta \log S_\nu / \Delta \log \nu \simeq 0$), interpreted as arising from a collimated, self-absorbed compact jet, in analogy to those observed in active galactic nuclei (Blandford & Königl 1979). With the direct imaging of a resolved compact radio jet from the core of Cygnus X-1 (Stirling et al. 2001), this association has been confirmed. Radio emission from X-ray binaries, especially the BHCs, is increasingly interpreted as the radiative signature of jet-like outflows.
It has been generally accepted that the soft thermal component of BH spectra originates in an optically thick, geometrically thin accretion disc (Shakura & Sunyaev 1973), whereas the power law component is produced by Comptonization of 'seed' photons in a hot, rarefied 'corona' of (quasi-) thermal electrons (Shapiro, Lightman & Eardley 1976; Sunyaev & Titarchuk 1980; Haardt & Maraschi 1991; Poutanen & Svensson 1996). Although this picture can successfully reproduce the X-ray behaviour, it can not yet address the clear correlation between radio and X-ray emission established for the persistent BHCs GX 339-4 and Cygnus X-1 while in the hard state (Hannikainen et al. 1998; Brocksopp et al. 1999; Corbel et al. 2000; Corbel et al. 2003). Moreover, some hard state sources, like XTE J1118+480 and GX 339-4, show evidence for a turnover in the infrared-optical band, where the flat-to-inverted radio spectrum seems to connect to an optically thin component extending up to the X-rays (Corbel & Fender 2002; Markoff et al. 2003a,b and references therein), suggesting again that the jet plays a role at higher frequencies.

Hence, all the evidence points to the corona in these systems being physically related to the presence of a jet: by far the simplest interpretation therefore is that the Comptonizing region is just the base of the relativistic outflow (Fender et al. 1999b; Merloni & Fabian 2002; Markoff et al. 2003a). However, joining these two previously independent scenarios is somewhat problematic because they often require different electron distributions and geometries.
Due to the fast timescales in X-ray binary systems, only simultaneous radio and X-ray observations provide the necessary tools to probe this conjecture. The following results extend and complete those presented in Gallo, Fender & Pooley (2002).

Table 2.1: System parameters for the ten hard state BHCs under consideration. Distance and $N_{\rm H}$ references are given in parentheses next to each value. Inclination and BH mass estimates, unless differently specified, are all taken from Orosz (2002). The last column refers to the literatures' sources from which we have obtained (quasi-) simultaneous radio and X-ray fluxes; no reference appears in case of our own observations (Cygnus X-1).

Source	Dist. (kpc)	Incl. (degree)	BH mass ($M_\odot$)	$N_{\rm H}$(ref) (10^{21}cm^{-2})	Data
Cygnus X–1	2.1 (1)	35±5	6.85–13.25	6.2 (16)	–
V 404 Cygni	3.5 (2)	56±4	10.06–13.38	5.0 (17)	21,22
GRS 1758–258	8.5 (3)	?	∼8–9 (14)	14.0 (3)	23
XTE J1118+480	1.8 (4)	81±2	6.48–7.19	0.1 (18)	24,25
GRO J0422+32	2.4 (5)	44±2	3.66–4.97	2.0 (5)	24
GX 339–4	4.0 (6)	15–60 (13)	5.8±0.5 (15)	6.0 (6)	26
1E 1740.7–2942	8.5 (7)	?	?	118 (19)	27
XTE J1550–564	4.0 (8,9*)	72±5	8.36–10.76	8.5 (20)	20,28
GS 1354–64	10.0 (10)	?	?	32.0 (9)	29
4U 1543–47	9.0 (11)	20.7±1.5	8.45–10.39	3.5 (11)	30

References : 1: Massey et al. 1995; **2:** Zycki, Done & Smith 1999; **3:** Main et al. 1999; **4:** McClintock et al. 2001; **5:** Shrader et al. 1997; **6:** Zdziarski et al. 1998; **7:** Sunyaev et al. 1991; **8:** Kong et al. 2002; **9:** Tomsick et al. 2001; **10:** Kitamoto et al. 1990; **11:** Orosz et al. 1998; **12:** Orosz 2002; **13:** Cowley et al. 2002; **14:** Keck et al. 2001; **15:** Hynes et al. 2003; **16:** Schulz et al. 2002; **17:** Wagner et al. 1994; **18:** Dubus et al. 2001; **19:** Gallo & Fender 2002; **20:** Tomsick et al. 2001; **21:** Han & Hjellming 1992; **22:** Hjellming et al. 2000; **23:** Lin et al. 2000; **24:** Brocksopp et al. 2003; **25:** Markoff, Falcke & Fender 2001; **26:** Corbel et al. 2000; **27:** Heindl, Prince & Grunsfeld 1994; **28:** Corbel et al. 2001; **29:** Brocksopp et al. 2001; **30:** Brocksopp, private communication.

*For XTE J1550–564 a distance of 4 kpc is assumed by both Kong et al. (2002) and Tomsick et al. (2001), as average value between 2.5 and 6 kpc, given by Sánchez-Fernández et al. (1999) and Sobczak et al. (1999) respectively.

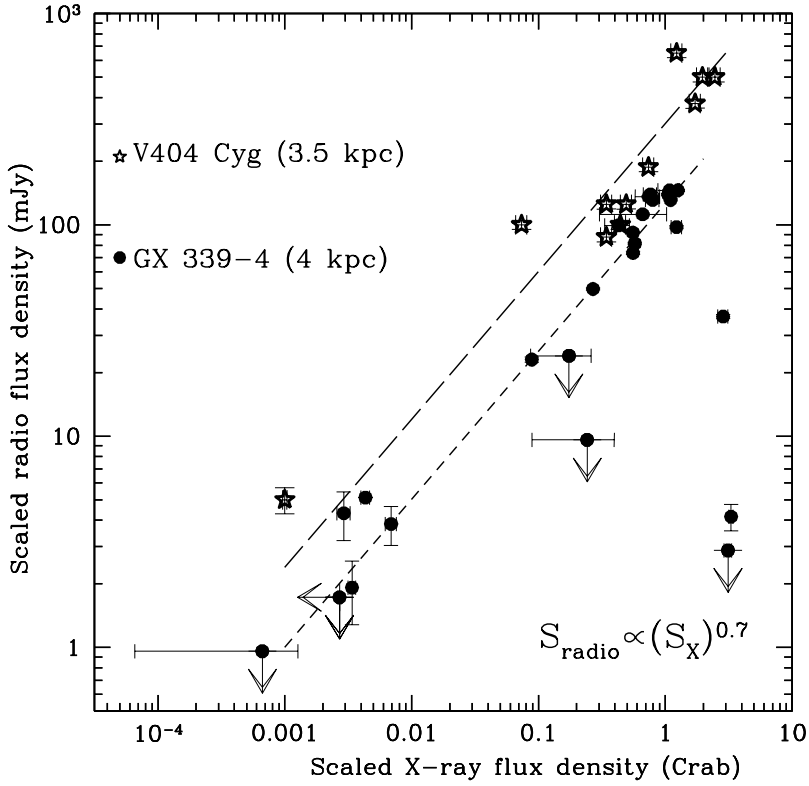

Figure 2.1: Radio against X-ray flux density, scaled to a distance of 1 kpc and absorption corrected, for V 404 Cygni and GX 339–4. Lines denote the fits to the datasets: short and long dashed for GX 339–4 and V 404 Cygni respectively. It is found that the data of V 404 Cygni are well fitted by the same functional relationship reported by Corbel et al. (2003) for the BHC GX 339–4, that is $S_{\rm radio} \propto (S_{\rm X})^{0.7}$.

2.2 The sample

Our aim was to compile (quasi-)simultaneous radio and X-ray observations of BHCs during the low/hard state. To this purpose, we have collected all the available (to our knowledge) data from the literature and made use of our own simultaneous observations as well. These were taken with the Ryle telescope at 15 GHz (see Pooley & Fender 1997 for more details) and combined with one-day averages from RXTE ASM (this refers to Cygnus X–1, Cygnus X–3 and GRS 1915+105). Table 2.1 lists the information for the ten low/hard state BHCs for which we have at our disposal (quasi-)simultaneous radio and X-ray coverage (see Section 2.5, Table 2.3 for 'non-canonical' hard state sources, such as Cygnus X–3 and GRS 1915+105): distance, mass, orbital inclination, measured hydrogen column densities (see Section 2.2.1) and literature references.
Both the X-ray and the radio intensity values come from several different instruments and telescopes. Radio flux densities have been measured in different frequency bands, ranging from 4.9 up to 15 GHz; nevertheless we generically refer to 'radio flux densities' based on the evidence that, while in the low/hard state, black hole radio spectra are characterised by almost flat spectra ($\alpha \sim 0$) spectral index (Fender 2001a).
X-ray fluxes, taken either from spectral fits or from light curves, have been converted into Crab units in order to be easily compared with radio flux density units (1 Crab $\simeq$ 1060 μJy; energy range 2–11 keV). For this purpose, X-ray fluxes/luminosities in a given range have been first converted into corresponding values between 2–11 keV, and then expressed as flux density. For those sources whose X-ray flux has been derived from count rates, the conversion into Crab has been performed according to the factors provided by Brocksopp, Bandyopadhyay & Fender (2003).

2.2.1 Absorption corrections

Whenever X-ray flux density has been evaluated from count rates or absorbed fluxes, we wanted to compensate for absorption by calculating the ratio between the predicted flux from a hard state BH with a measured $N_{\rm H}$ value, and the predicted flux corresponding to no absorption, as follows. We have first simulated with XSPEC typical spectra of hard state BHCs as observed by *Chandra* ACIS for ten different values of hydrogen column density ranging from zero up to 12.5 $\times 10^{22}$ cm^{-2}. A 'typical' spectrally hard BH's spectrum is well fitted by an absorbed power law with photon index 1.5. By keeping fixed the flux corresponding to no absorption, the points turn out to be well fitted by a simple

exponential relation, which allows to express the ratio $F_{\rm abs}/F_{\rm unabs}$ as follows:

$$\frac{F_{\rm abs,LS}}{F_{\rm unabs}} = \exp\left[\frac{-(N_{\rm H}/10^{22}{\rm cm}^{-2})}{18.38}\right] \tag{2.1}$$

The procedure described has been applied to X-ray fluxes below the transition luminosity between hard and soft state. Above that value, the spectrum is not reproduced by a simple power law. In this regime, the X-ray spectrum is usually well fitted by an absorbed power law with photon index $\Gamma \simeq 2.4$ plus a disc blackbody component, with a typical temperature of around 1 keV. Since in this case the 2–11 keV spectrum is almost entirely dominated by thermal emission, the previous simulations have been repeated for soft state BHCs by approximating the spectrum with a disc blackbody emission at 1 keV. We have obtained:

$$\frac{F_{\rm abs,HS}}{F_{\rm unabs}} = \exp\left[\frac{-(N_{\rm H}/10^{22}{\rm cm}^{-2})}{8.67}\right] \tag{2.2}$$

The latter correction has been applied to detections above the hard-to-soft state transition.

2.3 Radio vs. X-ray flux densities

2.3.1 GX 339–4 and V 404 Cygni

In Figure 2.1 we plot radio against X-ray flux densities (mJy vs.Crab), scaled to a distance of 1 kpc and absorption corrected, for GX 339–4 and V 404 Cygni, the two sources for which we have at our disposal the widest coverage in terms of X-ray luminosity.

GX 339–4 was discovered as a radio source by Sood & Campbell-Wilson (1994). When in the low/hard state, it is characterised by a flat or slightly inverted ($\alpha \gtrsim 0$) radio spectrum (see Corbel et al. 2000) and its synchrotron power has been shown to correlate with soft and hard X-ray fluxes (Hannikainen et al. 1998; Corbel et al. 2000). By means of simultaneous radio:X-ray observations of GX 339–4, Corbel et al. (2003) have recently found extremely interesting correlations between these two bands: in particular, $S_{8.6\ {\rm GHz}} \propto S_{3-9\ {\rm keV}}^{+0.71\pm0.01}$ (where S denotes the monochromatic flux, or 'flux density'; slightly different slopes – within the hard state – have been found depending on the X-ray energy interval). When fitted in mJy vs. Crab (scaled to 1 kpc and absorption corrected), the relation displays the form:

$$S_{\rm radio} = k_{\rm GX339-4} \times (S_{\rm X})^{+0.71\pm0.01} \tag{2.3}$$
$$k_{\rm GX339-4} = 126 \pm 3$$

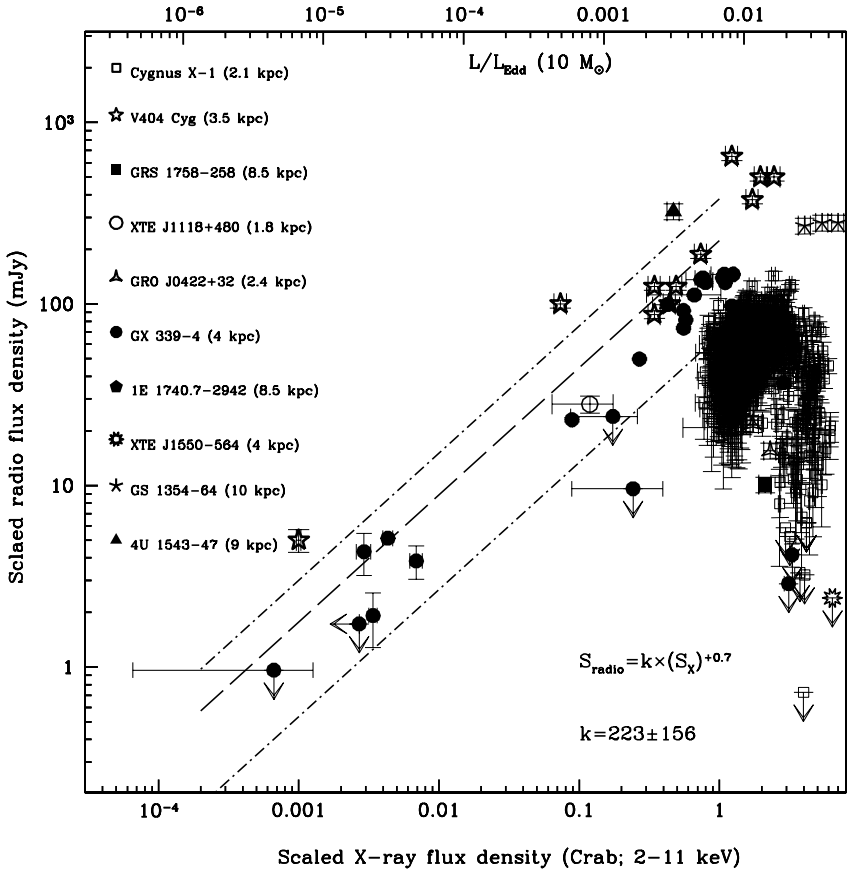

Figure 2.2: Radio flux density (mJy) is plotted against X-ray flux density (Crab) for a sample of ten hard state BHs (see Table 2.1), scaled to a distance of 1 kpc and absorption corrected (this means that the axes are proportional to *luminosities*). On the top horizontal axis we indicate luminosity, in Eddington units for a 10 $M_{\odot}$ BH, corresponding to the underlying X-ray flux density. An evident correlation between these two bands appears and holds over more than three orders of magnitude in luminosity. The dashed line indicates the best-fit to the correlation, that is $S_{\rm radio} = k \times (S_{\rm X})^{+0.7}$, with $k = 223 \pm 156$ (obtained by fixing the slope at +0.7, as found individually for both GX 339–4 and V 404 Cygni; see Section 2.4.1). Errors are given at 3–σ confidence level, and arrows also represent 3–σ upper limits.

The correlation appears to hold over a period of three years – 1997 and between 1999–2000 – during which the source remained almost constantly in a spectral hard state (with a transition to the high/soft state, Belloni et al. 1999, when the radio emission declined below detectable levels). Figure 2.1 shows radio against X-ray flux densities of GX 339–4 corresponding to simultaneous ATCA/RXTE observations performed between 1997 and 2000 (Corbel et al. 2000, 2003). Note that points above 1 Crab (scaled), which all correspond to RXTE-ASM detections, clearly show a sharp decreasing in the radio power (see next Section). The correlation reported by Corbel et al. (2003) actually refers to RXTE-PCA data only; it is worth mentioning that, when ASM detections below 1 Crab (*i.e.* below the radio quenching) are fitted together with PCA points, the final result is consistent, within the errors, with the fit reported by Corbel on PCA data alone (that is, a slope of 0.70±0.06 is obtained in this case).

Remarkably, we have found that detections of V 404 Cygni, the source for which we have at our disposal the widest radio:X-ray coverage, are well fitted by the same functional relationship – albeit with no apparent cutoff – as GX 339–4 (see Figure 2.1).
V 404 Cygni belongs to the class of X-ray transients, sources undergoing brief episodic outbursts during which their luminosity can increase by a factor $\sim 10^6$ compared to periods of relative quiescence. All V 404 Cygni data – except for the lowest quiescent point – come from simultaneous radio (VLA; Han & Hjellming 1992) and X-ray (*Ginga*; Kitamoto et al. 1990) observations during the decay following its May 1989 outburst, during which the source, despite very high and apparently saturated luminosity, never entered a spectral soft state and always maintained a very hard X-ray spectrum (Zycki, Done & Smith 1999). According to Hjellming et al. (2000), the quiescent state of V 404 Cygni, since it ended the long decay after its 1989 outburst, has been associated with a 0.4 mJy radio source[1]. Quiescent X-ray flux refers to a 1992 measurement (Wagner et al. 1994 report 0.024±0.001 count s^{-1} with ROSAT-PSPC), *i.e.* well before the onset of significant X-ray variability (see Kong et al. 2002 for details).
Denoting $S_{\rm radio}$ as the radio flux density in mJy and $S_{\rm X}$ as the X-ray flux density in Crab, we have obtained:

$$S_{\rm radio} = k_{\rm V404} \times (S_{\rm X})^{+0.70\pm0.20} \qquad (2.4)$$
$$k_{\rm V404} = 301 \pm 43$$

[1]Starting in early 1999, VLA obervations showed fluctuations ranging from 0.1 to 0.8 mJy on time scales of days; even more extreme radio fluctuations in February 2000 were accompanied by strong variability in the X-ray band as well (Hjellming et al. 2000).

The Spearman's rank correlation coefficient is 0.91; the two sided significance of its deviation from zero equals 4.2×10^{-3}.

These results indicate that $S_{\rm radio} \propto (S_{\rm X})^{\sim 0.7}$ is a fundamental property of the radio:X-ray coupling in the hard state, rather than a peculiarity of GX 339–4. It is worth stressing that the fitted slopes for V 404 Cygni and GX 339–4 are identical within the errors, with the same normalisations within a factor 2.5, while detections from other sources below 1 Crab (scaled), although much narrower luminosity ranges, are all consistent with the same placing in the radio:X-ray plane, as discussed in the next Section.

2.3.2 Broad properties of the correlation

In Figure 2.2 we plot radio flux densities (mJy) against X-ray fluxes (Crab), scaled to a distance of 1 kpc and absorption corrected, for all the ten hard state BHCs listed in Table 2.1. Note that this scaling and correction means that the axes are proportional to *luminosities*.
Besides GX 339–4, Cygnus X–1 displays a positive $S_{\rm radio} : S_{\rm X}$ correlation followed by a radio turnover around 3 Crab, whereas three other sources, namely XTE J1118+480, 4U 1543–47 and GS 1354–64, lie very close to the relations inferred for GX 339–4 and V 404 Cygni. The remaining four systems (GRS 1758–258, GRO J0422+32, 1E 1740.7–2942 and XTE J1550–564) seem instead to have already undergone the radio quenching.
We can assert that these ten BH candidates display very similar behaviour in the $S_{\rm radio}$ vs. $S_{\rm X}$ plane. There is evidence for a positive radio:X-ray correlation over more than three orders of magnitude in terms of Eddington luminosity, as indicated in the top horizontal axis, where we show the $L/L_{\rm Edd}$ ratio corresponding to the underlying X-ray flux ($L_{\rm Edd} \simeq 1.3 \times 10^{39}$ erg s^{-1} for a 10 $M_{\odot}$BH). As an example, the total luminosity of Cygnus X–1 in the 0.1 to 200 keV band, while the source is in the low/hard state, is $\sim 2\%$ of the Eddington luminosity for a 10 $M_{\odot}$ BH (di Salvo et al. 2001); that corresponds to mean flux of about 2.5 Crab (scaled to 1 kpc).

2.3.3 Jet suppression in the soft state

As already mentioned, approaching the soft state radio emission from BHCs seems to be quenched below detectable levels. Such a behaviour is well recognizable in at least two sources of our sample. As visible in Figure 2.2, both Cygnus X–1 and GX 339–4 display a clear turnover after which the radio power dramatically declines and reaches undetectable levels within a factor of two in

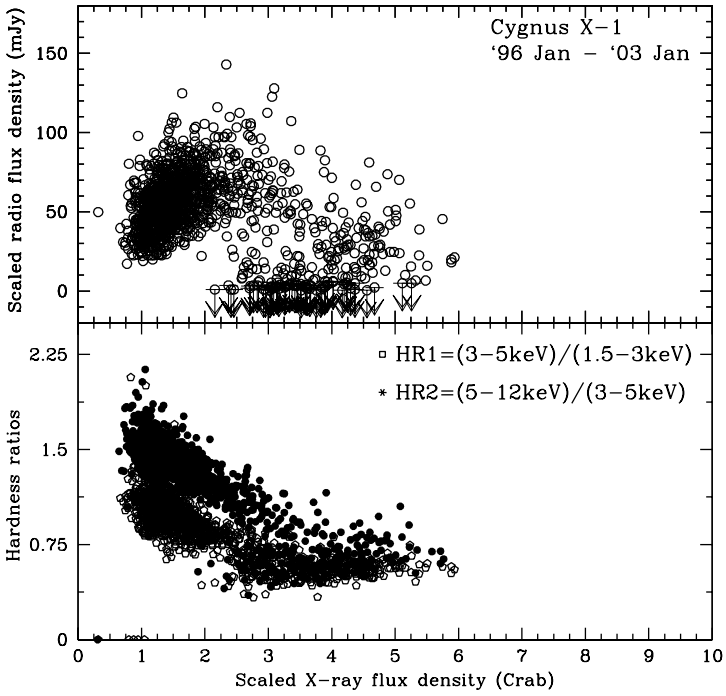

Figure 2.3: Top panel: Ryle telescope at 15 GHz and RXTE ASM daily averages for Cygnus X-1 between January 1996 and January 2003. Fluxes have been scaled to a distance of 1 kpc. Bottom panel: open squares for HR (Hardness ratio)1, defined as the ratio between the count rates at 3–5 keV and 1.5–3 keV. Filled circles for HR2, defined as the ratio between 5–12 keV and 3–5 keV. A softening of the X-ray spectrum is shown to correspond to a quenching in the radio emission.

X-ray flux (see also Fender et al. 1999b). In addition, XTE J1550–564, although suffering from poor statistics and large uncertainty in distance estimates (2.5–6 kpc), has been detected during the hard state (Corbel et al. 2001; Tomsick et al. 2001) at 'half-quenched' level (about 1 Crab:20 mJy scaled) while the radio emission dropped down significantly in the intermediate/very high state (about 6 Crab:<0.15 mJy scaled).
The values of the X-ray flux density (scaled) corresponding to the turnover in radio flux vary between the sources: GX 339–4, about 1 Crab; Cygnus X–1, about 3 Crab; V 404 Cygni > 1 Crab. This difference could be related to differences between the parameters that govern the powering/quenching mechanism(s) of the radio emitting jet. A discriminant parameter might be the BH mass, which is estimated to be ~10 $M_{\odot}$ in the case of Cygnus X–1 while it has been recently constrained around 6 $M_{\odot}$ in the case of GX 339–4 (Hynes et al. 2003). If this hypothesis is correct, we would expect not to see jet quenching at X-ray luminosities below the Cygnus X–1 turnover for those systems whose BH mass has been estimated to be bigger than 10 $M_{\odot}$, as, for instance, the case of V 404 Cygni, which does not appear to be quenched in radio up to about 3 Crab, and is known to possess a 10–14 $M_{\odot}$ BH (Orosz 2002, Hjellming et al. 2000). Despite the poor statistics, this picture seems to bear out the hypothesis that the X-ray luminosity at the radio quenching might positively correlate with the BH mass, being consistent with the jet suppression occurring at a constant fraction – a few percent – of the Eddington rate.
In Figure 2.3 the quenching of the radio power in Cygnus X–1 (monitored simultaneously in radio and X-ray between January 1996 and January 2003) as a function of the X-ray flux density is shown together with X-ray hardness ratios. The 3–12 keV X-ray spectrum softens until about 5 Crab (scaled), whereas radio quenching begins around 3 Crab (scaled). While it is clear that the quenching occurs somewhere near the point of transition from low/hard to softer (intermediate or high/soft) states, pointed observations will be required to see exactly what is happening to the X-ray spectrum *at* the quenching point.

2.4 Spread to the correlation

2.4.1 Best–fitting

So far we have established two main points by looking at the distribution of low/hard state BH binaries in the radio vs. X-ray flux density plane:

- Independently of the physical interpretation, $S_{\rm radio} \propto (S_{\rm X})^{+0.7}$ for GX

339–4 and V 404 Cygni from quiescence up to close to the hard–to–soft state transition. All other hard state BHCs lie very close to these correlations, with similar normalisations.

- At a luminosity of a few percent of the Eddington rate, close to the hard–to–soft state transition, a sharp turnover is observed in the radio:X-ray relation, that is, the radio flux density drops below detectable levels.

Bearing this in mind, our purpose is now trying to find a reliable expression for a 'best–fit' relationship to all hard state BHs and to estimate the spread relative to such a relation.
Assuming 0.7 as a universal slope during the low/hard state, we have determined the normalisation factor by fitting all the data – Cygnus X–1 excluded (see comments at the end of this Section) – up to 1 Crab, below which quenching does not occur for any system.
In this way we are able to provide an empirical relationship valid for all the hard state BHs, that we will call 'best–fit' in the following. We have obtained:

$$S_{\rm radio} = k \times (S_{\rm X})^{+0.7}, \qquad k = 223 \pm 156 \tag{2.5}$$

The best–fit and its spread are indicated in Figure 2.2 in dashed and dot–dashed lines respectively. A scatter of about one order of magnitude in radio power is particularly interesting, especially in view of comparing the observed spread to the one we expect based on beaming effects (see next Section).

The choice of excluding the whole dataset of Cygnus X–1 is related to its unusual behaviour in the radio:X-ray flux plane. In fact, a visual inspection of Figure 2.2 already suggested that the points below the radio power quenching belong to a line with a steeper slope than 0.7. In addition, despite its relatively low inclination to the line of sight (see next Section for clarity), Cygnus X–1 lies on the lower side of the correlation. It is possible that these characteristics can be explained in terms of strong wind absorption. It has been demonstrated that the wind from the donor OB star in Cygnus X–1 partially absorbs the radio emission, up to about 10% (Pooley, Fender & Brocksopp, 1999; Brocksopp, Fender & Pooley, 2002). In addition, since the jet bulk velocity during hard state is likely to be relatively low, approaching and receding jets contribute a similar amount to the total radio luminosity. However, in Cygnus X–1 only a one–sided jet has been detected (Stirling et al. 2001); this means that, possibly, a significant fraction of the receding jet is lost through wind absorption (however, since the jet structure is about 100 times bigger than the orbit, it is unlikely that the wind could absorb the entire power of the receding component). Furthermore,

because the flat–spectrum radio emission (corresponding to steady jet and generally associated with hard X-ray spectrum) is optically thick, this implies that when the jet power decreases, its size might also decreases linearly with flux. As the jet in Cygnus X–1 becomes smaller, the $S_{\rm radio}$:$S_{\rm X}$ relation will be subject to increasingly strong wind absorption, with the net result of steepening the correlation.

2.4.2 Constraining the Doppler factors

What kind of physical information can we deduce from the observed relation? Let us assume a very simple model, in which the same physics and jet/corona coupling hold for all hard state BHs and the observed functional relationship is intrinsic; then, one would predict the following placing in the $S_{\rm radio}$ vs. $S_{\rm X}$ parameter space:

1. All sources lying on a line with the same slope if neither X-ray or radio emission were significantly beamed (*i.e.* low Doppler factors).

2. Different sources lying on lines with the same slope but different normalisations if X-rays were isotropic while radio was beamed, with radio–brighter sources corresponding to higher Doppler factors.

3. As point (ii) but with higher Doppler factors sources being brighter in both radio and X-ray if both were beamed.

Despite the relatively small sample, we are able to place some constraints on these possibilities. In the first two scenarios, where X-rays are isotropically emitted while radio power is beamed, we can express the observed radio luminosity as the product of the intrinsic (rest–frame) radio power times the effective Doppler factor $\Delta_{\rm radio}$, defined as a function of approaching and receding Doppler factors[2]. If $S_{\rm radio,intr} = k \times (S_{\rm X})^{+0.7}$ for all hard state BHCs, we can write:

$$S_{\rm radio,obs} = \Delta_{\rm radio} \times S_{\rm radio,intr} = \Delta_{\rm radio} \times N \times (S_X)^{+0.7} \qquad (2.6)$$

Assuming the same coupling for all sources – that means same normalisation N – the ratio $S_{\rm radio,1}/S_{\rm radio,2}$ between the observed radio powers from source 1 and 2, at a fixed X-ray luminosity, will correspond to the ratio between their relative effective Doppler factors.

[2] $\Delta_{\rm radio} := [(\delta_{\rm app})^2 + (\delta_{\rm rec})^2]/2$, where: $\delta_{\rm rec/app} = \Gamma^{-1} \times (1 \pm \beta\cos\theta)^{-1}$; $\beta = v/c$, is the bulk velocity of the radio–emitting material; $\Gamma = (1-\beta^2)^{-0.5}$; θ is the inclination respect to the line of sight.

Returning to the case of V 404 Cygni and GX 339–4, where $S_{\rm radio,V404}/S_{\rm radio,GX339-4} \sim 2.5$, we are drawn to the conclusion that GX 339–4, whose inclination is poorly constrained between $15 < i < 60°$ (Cowley et al. 2002), is likely to be located at a higher inclination than V 404 Cyg, well established to lie at $56 \pm 4°$ (Shahbaz et al. 1994). In fact, assuming that $\Gamma_{\rm GX339-4} \simeq \Gamma_{\rm V404}$, a ratio $S_{\rm radio,V404}/S_{\rm radio,GX339-4} > 1$ can be achieved only if $i_{\rm GX339-4} > i_{\rm V404}$.

Clearly, the previous arguments are based on the assumption that the binary system inclination to the line of sight coincides with the inclination of the jet, while recent findings (Maccarone 2002) show that this is not always the case (the misalignment of the disc and the jet has been already observed in Galactic jet sources GRO J1655–40 and SAX J1819–2525).
A recent work by Hynes et al. (2003) shows dynamical evidence for GX 339–4 being a binary system hosting a BH with mass $5.8 \pm 0.5 \ M_{\odot}$. Interestingly, based on the spectroscopic analysis by Cowley et al. (2002), see their Figure 8, this value is also consistent with a high inclination of the system to the line of sight.

Monte Carlo simulations I: radio beaming

In order to link the measured scatter in the radio:X-ray relation to the beaming effects, and possibly constraining the Doppler factors, we have performed Monte Carlo simulations according to the following scheme. We have considered the four sources (see Table 2.2) whose radio:X-ray flux densities have been utilised to obtain the best–fit relationship below 1 Crab; for each of them we have at our disposal a number $n_{\rm j}$ of simultaneous detections, with a total number of points $n = \Sigma_{\rm j=1}^{4} n_{\rm j} = 23$. For each source j, a random inclination within the measured range has been generated and associated to an array whose dimension equals the number of detections $n_{\rm j}$, for a total of 23 random inclinations. Then, for 15 different values of the outflow bulk velocity β, the corresponding Doppler factors $\Delta_{\beta}(j)$ have been calculated by running the simulation 10^4 times (*i.e.* for total of 23×10^4 values for each β) . After estimating the mean Doppler factor and its relative standard deviations ($\sigma(\Delta)$) for each value of β, we have compared the simulated spread (defined as the ratio $\sigma(\Delta)/\Delta_{mean}$ to the measured spread in normalisation, that is $\sigma(k)/k = 156/223 = 0.70$).

The result is shown in Figure 2.4: in order to keep the spread in Doppler

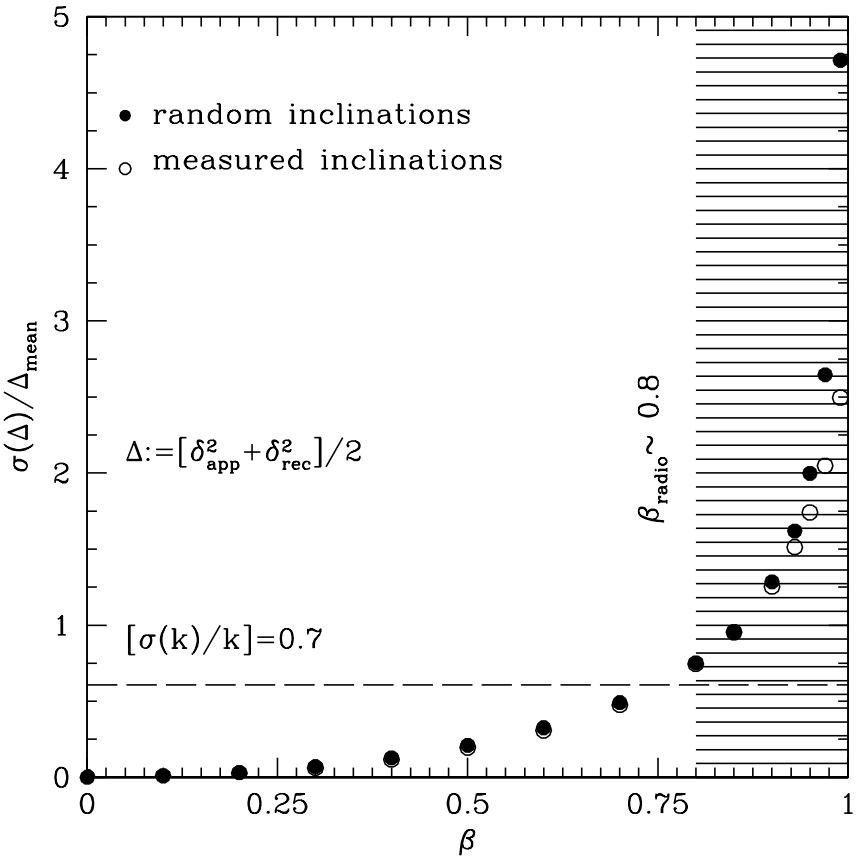

Figure 2.4: Assuming a simple model in which radio emission is beamed while X-rays are isotropic, equation 2.6 implies that the spread in radio power to the best fit can be due to the distribution in Doppler factors. The simulated spread in Δ_{radio} (defined as the ratio of standard deviation over the mean value), is plotted for 15 values of the jet bulk velocity between 0 and 0.998c, and compared to the measured scatter in the radio:X-ray correlation. In order to maintain the spread in Doppler factors equal/smaller than observed, the outflow velocity must be smaller than 0.8 times the speed of the light, that is $\Gamma_{radio} < 1.7$. Filled circles represent Monte Carlo simulation run by allowing the inclination angles to vary between 0–90° ; open circles correspond to the measured inclination angles.

Table 2.2: Observed sources for which mean Doppler factors have been simulated for 10 different values of the jet bulk velocity; measured range of inclinations and number of simultaneous radio:X-ray detections are listed.

Source	Inclination (degree)	Number of detections (n_j)
V 404 Cygni	56 ± 4^a	7
XTE J1118+480	81 ± 2^a	1*
4U 1543–47	20.7 ± 1.5^a	1
GX 339–4	$15–60^b$	14

* This single point corresponds to the average of 33 nearly simultaneous detections over a very narrow interval in X-ray luminosity.
References: a: Orosz 2002; **b:** Cowley et al. 2002.

factor equal/smaller [3] than observed (actually $\leq 0.77 = 0.70 + 10\%$), the bulk velocity of the radio–emitting material must be lower than $0.8c$, that is the Lorentz factor must be smaller than 1.7.

These remarks are of course valid under the basic assumptions that no beaming is affecting the X-rays. In addition we are considering a simple model in which both the bulk velocities and opening angles of the jets are constant (only under the latter assumption the probability of observing a source with a given inclination θ is uniformly distributed in $\cos\theta$).

For comparison, we ran the simulation allowing the inclination angles to vary between 0–90° (filled circles in Figure 2.4); this is actually important in the light of what has been discussed by Maccarone (2002) about jet–disc misalignment in BH binaries, and also takes into account possible model–dependent errors in the estimation of i. The simulated spread in Doppler factors starts to significantly deviate from the previous one (calculated allowing the inclination angles for each source to vary within the measured values; open circles in Figure 2.4) only for very high bulk velocities. As expected, even if inclinations

[3] Smaller than measured spread are also 'allowed' on the ground that errors in the distance estimates are likely to influence the observed distribution, causing an additional source of scatter to the relation, which is of course not related to any boosting effect.

as 0 and 90° (*i.e.* those inclinations which translate into the highest and lowest possible values of cosine, respectively) are also taken into account, this strongly influences the mean Doppler factor only for really high values of β.

Monte Carlo simulations II: adding beamed X-rays

Following a similar approach, it is possible to constrain the Doppler factor due to the combination of beamed radio *and* X-ray radiation. As before, we assume 0.7 as an intrinsic slope which relates radio and X-ray emission. Supposing that both X-rays and radio are beamed, we will write:

$$\frac{S_{\mathrm{radio,obs}}}{(S_{\mathrm{X,obs}})^{0.7}} \propto \frac{\Delta_{\mathrm{radio}}}{(\Delta_{\mathrm{X}})^{0.7}} \tag{2.7}$$

Note that the effective Doppler factor for the X-ray radiation will be defined as $\Delta_{\mathrm{X}} = [(\delta_{\mathrm{rec}})^{2.5} + (\delta_{\mathrm{app}})^{2.5}]/2$ (assuming continuous ejection and photon index 1.5 for low/hard state; see Mirabel & Rodríguez 1994, equations 8, 9).
Therefore, Monte Carlo simulations have been run by varying both radio and X-ray bulk velocities with logarithmic steps in Lorentz factors, Γ_{X} and Γ_{radio}, between 1 and 30.
The mean values of $\Delta_{\mathrm{radio}}/(\Delta_{\mathrm{X}})^{0.7}$ together with their standard deviations and spreads have been calculated for any combination of the two factors. The results are shown in Figure 2.5.
Filled bold circles indicate those combinations of Γ_{radio} and Γ_{X} for which the simulated spread with inclinations varying between 0–90° is smaller than/equal to 0.77. Filled-plus-open circles, instead, correspond to 'allowed' combinations when the inclination to the line of sight varies within the measured ranges.
In order to see why the beaming of both wavebands allows a wider spread of Γ, consider the effect on the position of a source in the flux–flux diagram: a Doppler–boosted, or deboosted, radio source moves parallel to the S_{radio} axis, while a source boosted or deboosted in both wavebands moves roughly (not exactly) parallel to the line $S_{\mathrm{radio}} = \mathrm{const} \times S_{\mathrm{X}}$, and therefore roughly along the direction of the observed correlation. Consequently beaming in both wavebands disturbs the correlation less. However, if X-rays were really highly beamed, that would imply strong X-ray selection effects in detecting BH binaries.
Clearly, a possible independent estimation of the bulk velocity of the X-ray emitting material (*e.g.* Beloborodov 1999; Maccarone 2003) would naturally allow a much narrower constraint on the Doppler factor of the radio–emitting material (see discussion for further details).

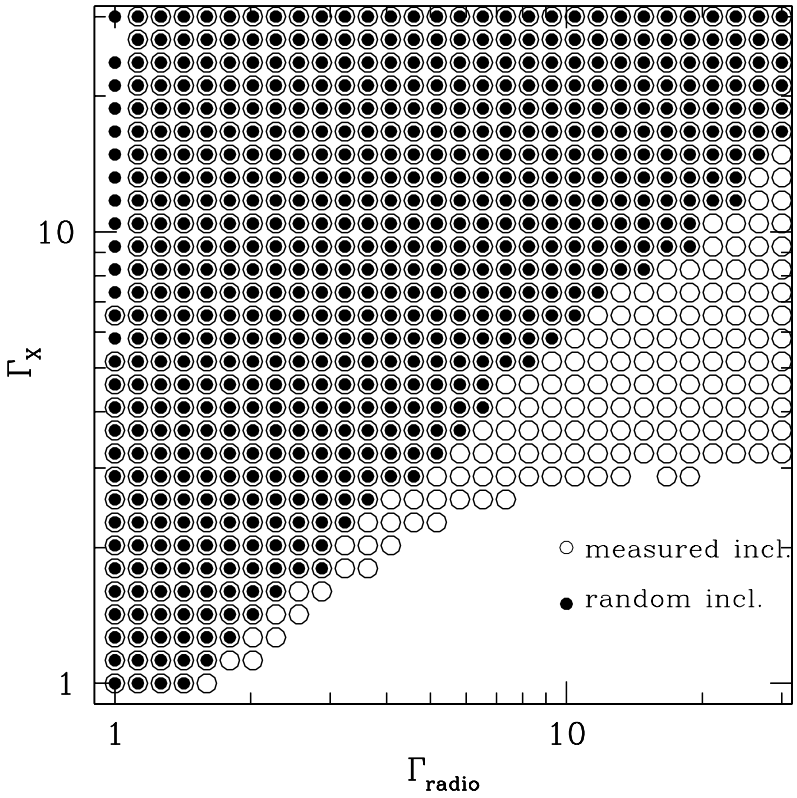

Figure 2.5: Same scheme as Figure 2.4, but assuming a model in which both radio and X-ray beaming are allowed; in this case, Monte Carlo simulations have been performed with logarithmic steps in Lorentz factors (rather than linear in β). The combination of radio plus X-ray beaming has the effect of broadening the range of allowed Γ_{radio} with respect to the case of isotropic X-ray emission. In this picture open circles indicate combinations of Γ_{radio} and Γ_X for which the simulated spread with inclinations varying within the measured ranges is smaller than/equal to 0.77. Filled circles, instead, correspond to 'allowed' combinations of Γ_{radio} and Γ_X when the inclination to the line of sight is randomly chosen between 0–90° . In this case the range of possible combination is smaller due to the fact that extreme inclinations, such as 0 or 90° are also taken into account.

2.5 Beyond the hard–to–soft state transition

2.5.1 Discrete ejections

So far, we only have focused on low/hard state BHs, that is, binary systems characterised by a quasi–steady state of stable accretion and whose X-ray spectrum is dominated by a hard power law.
In the following we will add to our sample radio and X-ray fluxes from transient BHCs during their episodic outbursts associated with discrete ejection events corresponding to optically thin radio emission.
All the available data, comprising of soft X-ray and radio peak fluxes with references, have been reported by Fender & Kuulkers (2001). Two points we include in this Section come from systems which have also been shown in Figure 2.2 while in the hard state, namely V 404 Cygni and GRO J0422+32. Sources under consideration, as well as their fundamental physical parameters, are listed in Table 2.3. Simultaneous radio:X-ray peak fluxes, scaled to a distance of 1 kpc are plotted in Figure 2.6 with filled squares.
Radio data are based on peak observed flux density at frequency of 5 GHz. Where measurements at 5 GHz were not available, a spectral index of $\alpha = -0.5$ was assumed in order to estimate the 5 GHz flux based on observations performed at different frequencies (see Fender & Kuulkers 2001 for details).
Most of the X-ray data are ASM detections, with the only exceptions of GRO J1655–40 and GRO J0422+32, whose outbursts have been detected by either BATSE or GRANAT. For clarity, no error bars are plotted.

2.5.2 Other BHCs: persistent soft state and 'extreme' sources

In between the jet quenching and the discrete ejections from transient sources, there are of course binary systems displaying a persistent soft spectrum, *i.e.* whose emission is dominated by disc blackbody photons. LMC X–1 and LMC X–3, in the Large Magellanic Clouds, are the only BHCs always observed while the soft state (actually Wilms et al. 2001; Boyd & Smale 2000 and Homan et al. 2000 reported signs that LMC X–3 entered a hard state). For both these sources, the presence of a black hole is quite well established, with a most likely mass of 9 $M_{\odot}$ and 6 $M_{\odot}$, respectively for LMC X–3 and LMC X–1. By means of radio and X-ray observations performed in 1997, we can place the two sources in the $S_{\rm radio}$ vs. $S_{\rm X}$ plane, in order to verify the amount of radio power from soft state BHs, which is expected to be well below the hard state correlation. LMC X–3 X-ray flux densities have been derived from Haardt et al. (2001), while LMC X–1 from Gierlinski et al. (2001). Radio upper limits for both sources are

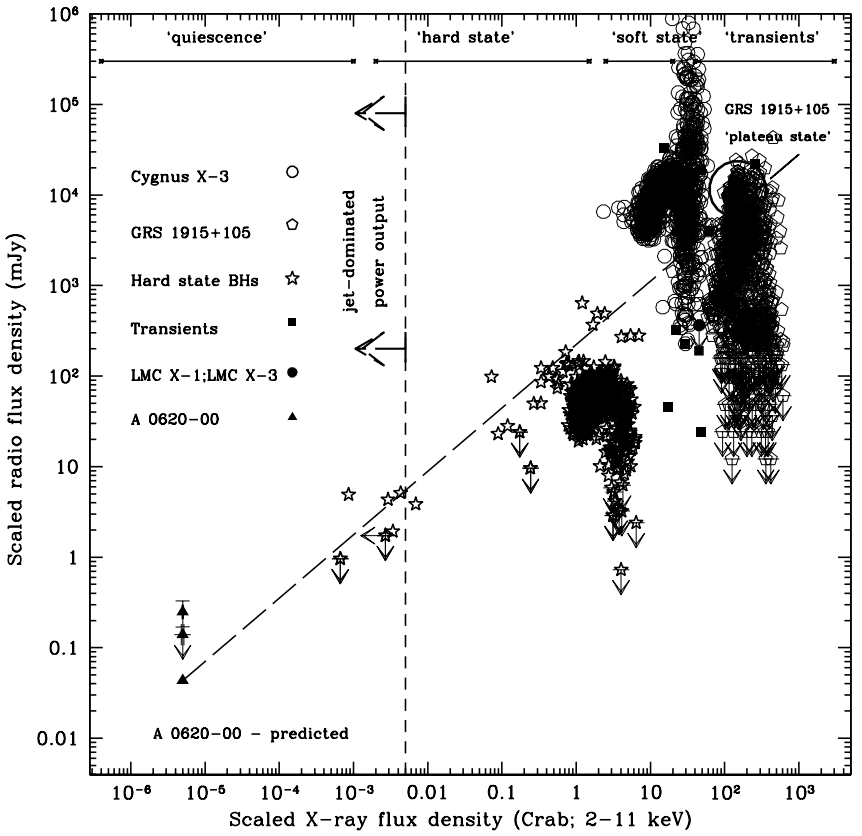

Figure 2.6: In addition to hard state BHs (open stars) we plot both single simultaneous radio:X-ray fluxes from black hole transients and detections from two canonical soft state plus somewhat 'extreme' sources, close to the Eddington accretion regime. Filled squares correspond to single outbursts from different sources (from Fender & Kuulkers 2001); filled circles are for persistent soft/high state sources LMC X–1 and LMC X–3, upper limits; open polygons refer to GRS 1915+105, while open circles denote Cygnus X–3 points. Based on the 0.7 correlation, and assuming that the radio luminosity scales as the total jet power raised to $x = 1.4$ (as in the Blandford & Königl, 1979, and MFF models), the radio luminosity is expected to dominate the X-rays below $L_{\rm X} \simeq 4 \times 10^{-5} {\rm L}_{\rm Edd}$ (about 0.005 Crab). Possible detection of the nearby SXT A 0620–00 at the predicted radio level would be capable to probe such a statement at very low X-ray level, requiring a wholly new accretion regime on to stellar BHs.

Table 2.3: Transient (plus 4 peculiar) sources whose simultaneous radio:X-ray peak fluxes associated with discrete ejections are plotted in Figure 2.6 (data from Fender & Kuulkers 2001).

Source	Distance (kpc)	$N_{\rm H}$ (10^{22} cm^{-2})
1A 0620–00	1 (1)	0.2 (a)
GS 2000+25	2 (2)	0.2 (b)
GS 1124–68	4.9 (3)	0.5 (c)
GRO J1655–40	3 (4)	0.7 (d)
GRS 1716–249	2.4 (5)	0.4 (e)
GRS 1739–278	8.5 (6)	2.6 (f)
4U 1630–472	10 (7)	9.4 (g)
XTE J2012+381	10 (8)	1.3 (h)
XTE J1748–288	8 (9)	7.5 (i)
XTE J1859+226	7.6 (10)	0.3 (l)
XTE J0421+560	5 (11)	0.1 (m)
GRS 1915+105	11 (12)	7.0 (n)
Cygnus X–3	9 (13)	2.7 (o)
LMC X–1	55 (14)	0.8 (14)
LMC X–3	55 (14)	0.1 (14)

References : 1: Shahbaz et al. 1994; **2:** Callanan et al. 1996; **3:** Shahbaz et al. 1997; **4:** Kubota et al. 2001; **5:** Della Valle et al. 1994; **6:** Martí et al. 1997 ; **7:** Parmar et al. 1986; **8:** Campana et al. 2002; **9:** Kotani et al. 2000; **10:** Hynes et al. 2002; **11:** Robinson et al. 2002; **12:** Fender et al. 1999a; **13:** Predehl et al. 2000; **14:** Haardt et al. 2001.

a: Kong et al. 2002; **b:** Rutledge et al. 1999; **c:** Ebisawa et al. 1994; **d:** Ueda et al. 1998; **e:** Tanaka 1993 **f:** Greiner et al. 1996; **g:** Tomsick & Kaaret 2000; **h:** Hynes et al. 1999; **i:** Miller et al. 2001; **l:** Markwardt et al. 1999; **m:** Parmar et al. 2000; **n:** Klein–Wolt et al. 2002; **o:** Terasawa & Nakamura 1995.

taken from Fender, Southwell & Tzioumis (1998). The corresponding values, scaled to a distance of 1 kpc and corrected for absorption according to equation 2, are plotted in Figure 2.6 with filled circles (at about 150 Crab:<4540 mJy and 45 Crab:<360 mJy, LMC X–1 and LMC X–3 respectively). As expected, both points lie below the hard state relation extended to such high X-ray energies. Although we are only reporting upper limits, we can assert that fluxes from LMC X–1 and LMC X–3 do not disagree with our previous finding.

For completeness, simultaneous radio:X-ray detections of two extreme sources, namely GRS 1915+105 (open polygons) and Cygnus X–3 (open circles), have been included, corresponding to the two big 'clouds' at the top right region of Figure 2.6. Both systems are traditionally considered 'exotic' due to their timing and spectral behaviour which do not fully resemble any 'standard' picture generally accepted for BHCs; for instance, both these sources display either optically thin or thick radio spectra. For extensive reviews, see Bonnet–Bidaud & Chardin (1988; Cygnus X–3) and Belloni et al. (2000; GRS 1915+105). Here we note that, despite its unusually high luminosity, detections of GRS 1915+105 in the so called *plateau state* (Belloni et al. 2000) – which appears to share similar properties with the canonical low/hard state – still seem to belong to the 0.7 correlation extended up to super–Eddington regime.

Cygnus X–3 is the strongest observed persistent radio–emitting BH binary and is embedded in a dense stellar wind from the companion Wolf–Rayet star (van Kerkwijk et al. 1992; Fender, Hanson & Pooley 1999), which makes it difficult to isolate the compact object high energy spectrum. The high energy emission from the vicinity of the compact object in Cygnus X–3 is likely to be hidden by a dense stellar environment surrounding the source; as a consequence, the intrinsic X-ray luminosity might be higher than inferred, pushing the dataset closer to the 0.7 relation. Moreover, there still remains uncertainty about the nature of the accretor in this system. The neutron star hypothesis can not be ruled out with confidence.
It is interesting to note that, while the jets from GRS 1915+105 are at 60–70° (Fender et al. 1999a), those of Cygnus X–3 appear to be close to the line of sight ($\lesssim 14°$, Mioduszewski et al. 2001), supporting the previous hypothesis, in which higher–than–average normalisation factors would correspond to higher Doppler factors. In addition, the behaviour of Cygnus X–3, with the apparent turnover in the radio power, is very similar to that of Cygnus X–1, except for the flaring behaviour following the jet quenching (note that points corresponding to this flaring show characteristic optically thin radio spectra; on the contrary,

Table 2.4: Five X-ray transients have been monitored in X-rays by different telescopes in different energy ranges (indicated below the table) during quiescence. Here we report the values for the maximum and the minimum luminosity, with relative references and energy ranges. For these values the corresponding predicted radio flux densities have been calculated based upon the radio:X-ray correlation we have found, that is $S_{\rm radio} = [223 \times (S_{\rm X,1kpc}/{\rm Crab})^{0.7}]/({\rm D/kpc})^2$ mJy.

Source	$L_{\rm X}$ (10^{32} erg s^{-1})	Distance (kpc)	$S_{\rm X}$ at 1 kpc (10^{-6}Crab)	Predicted radio flux (μJy)
1A 0620–00	0.02[1]– 0.04[2] (a,b)	1	1–5	18–43
GRO J1655–40	0.2[3]– 3[4] (a,c)	3	6–82	6–34
XTE J1550–564	< 5 [5] (d)	4	< 173	< 32
GRO J0422+32	0.08[4] (e)	2.4	∼ 2	∼4
GS 2000+25	0.02[4] (e)	2	∼ 0.5	∼2

References : 1: 0.4–2.4 keV; **2:** 0.4–1.4 keV; **3:** 0.3–7 keV; **4:** 0.5–10 keV; **5:** 0.5–7 keV. **a:** Kong et al. 2002; **b:** Narayan et al. 1996; **c:** Asai et al. 1998; **d:** Tomsick et al. 2001; **e:** Garcia et al. 2001.

pre–flaring detections display 'flat' radio spectra, *i.e.* a different physical origin).

2.6 Predicting radio fluxes at low quiescent luminosities

As the same correlation appears to be maintained over many years and for different sources (like for instance Cygnus X–1, GX 339–4, V 404 Cyg), we can estimate the level of radio emission from a hard state BH by measuring its X-ray flux alone. This is particularly interesting in the case of black hole X-ray transients, whose inferred accretion rate during quiescence may be very small.
Kong et al. (2002) present *Chandra X-ray Observatory* observations of three BH transients during quiescence for which no simultaneous radio detection is available to date, namely A 0620–00, GRO J1655–40 and XTE J1550–564. In order to check for possible spectral variability, they also report results from previous X-ray observations carried out by different telescopes, such as ROSAT, ASCA and *Beppo*-SAX. According to Tomsick et al. 2001, the lowest luminosity measured for XTE J1550–564 with Chandra (5×10^{32} erg s^{-1}, for a distance of 4 kpc) should however be considered only as an upper limit on the quiescent luminosity

of the system. *Chandra* detections of other two transient sources, namely GRO J0422+32 and GS 2000+25, are reported by Garcia et al. 2001. In Table 2.4 we list for each of the five sources the maximum and the minimum measured X-ray luminosity in quiescence, the inferred distance and the predicted radio flux density (in μJy) based on our best–fit equation, that is $S_{\rm radio} = 223 \times (S_{\rm X})^{+0.7}$. Given a spread of 156 over 223 in the normalisation factor, the predicted values must be considered reliable within one order of magnitude.

2.6.1 A 0620–00: the ideal candidate

The Soft X-ray Transient (SXT) A 0620–00 was discovered in outburst in 1975 (Elvis et al. 1975), while the associated radio source was at a level of 200–300 mJy (Owen et al. 1976) during the onset of the outburst. Six years later the source was detected with the VLA at level of 249 ± 79 μJy (Geldzahler 1983); additional VLA observations in 1986 (see McClintock et al. 1995) yielded an upper limit of 140 μJy, clearly indicating a decline in radio power (see Figure 2.6 where A 0620–00 detection/upper limit/predicted radio fluxes are marked with triangles). The 1981 detection might actually be associated to radio lobes resulting from the interaction of a relativistic–decelerating jet with the interstellar medium, as observed in the case of XTE J1550–564 about four years after the ejection of plasma from near the BH (Corbel et al. 2002).

Due to its relative proximity, A 0620–00 is the most suitable candidate to probe if our empirical radio:X-ray relation does hold down to low quiescent X-ray luminosity ($\simeq 2 \times 10^{30}$ erg s^{-1} at 1 kpc, *i.e.* about $10^{-8} L_{\rm Edd}$; Garcia et al. 2001). In other words, if A 0620–00 was detected at the predicted radio level (a few tens of μJy, see Figure 2.6, bottom left corner), it would confirm that the mechanisms at the origin of radio and X-ray emission are correlated, if not even partly coincident, over more than six orders of magnitude in X-ray luminosity.

Moreover, if the radio:X-ray correlation were confirmed at very low X-ray luminosities (below 10^{-4} $L_{\rm Edd}$) it would strongly constrain the overall theory of accretion in quiescence. We direct the reader to the discussion for further comments.

2.7 Discussion

The presence of a coupling between radio and X-ray emission in the low/hard state of black hole binaries obviously requires a theoretical interpretation that relates somehow the powering/quenching mechanism(s) of the jet to the overall accretion pattern. Zdziarski et al. (2003) ascribe the correlation to a correspondence between the level of X-ray emission and the rate of ejection of radio–emitting blobs forming a compact jet. In this picture, there still remains the question of the condition for jet suppression. Meier (2001) interprets the steady–jet/hard–X-ray state association as strong evidence for magnetohydrodynamic (MHD) jet formation, where the most powerful jets are the product of accretion flows characterised by large scale height. The simulations show in fact that the jet is confined by the toroidal component of the magnetic field lines, coiled due to the disc differential rotation: the bigger the disc scale–height, the stronger the field. The power of the jet naturally decreases (at least 100 times weaker) in the soft/high state, associated with a standard geometrically thin disc (Shakura & Sunyaev 1973).
To date, two broad classes of geometries have been proposed for explaining X-ray emission from low/hard state BHs. The more classical picture is that of a hot, homogeneous, optically thin corona of (quasi–)thermal electrons which inverse Compton scatter 'seed' photons coming from the underlying accretion disc (Shapiro, Lightman & Eardley 1973 and similar later solutions). The alternative is that of a jet–synchrotron model, in which, under reasonable assumption on the input power of the jet and the location of the first acceleration zone, optically thin synchrotron emission can dominate the X-ray spectrum, traditionally thought to be a product of inverse Compton process only (see Markoff, Falcke & Fender 2001 for a detailed description of the model; hereafter MFF). This model however predicts self–synchrotron Compton up-scattering in the jet for some scenarios. Interestingly the MFF model is able to reproduce the observed slope of the radio:X-ray correlation analytically (Markoff et al. 2003a), as a function of the measured X-ray and radio–infrared spectral indices.

A revised version of the classical Comptonization model for the hard state has been proposed by Beloborodov (1999). In this case the hot coronal plasma is powered by magnetic field line reconnections (Galeev, Rosner & Vaiana 1979) and confined within several active flares with mildly relativistic bulk velocities, inferred by the relative weakness of the reflection component. Due to aberration effects in fact, the amount of X-rays as seen by the reflecting disc turns out to be reduced by a factor consistent with $\beta_{\rm X} \simeq 0.3$.

Maccarone (2003) draws a similar conclusion on a different ground: he has tabulated all the the available measurements of X-ray luminosities at the time of the soft–to–hard state transition, for both BHC and neutron star systems. The resultant variance in state transition luminosity is also consistent with coming from material with $\beta_X \simeq 0.2$; therefore $\Gamma_X \simeq 1$ in both cases.
Following the approach of Section 2.4.2, this immediately implies a stringent upper limit on the beaming of radio emission as well, that is $\mathbf{\Gamma}_{\rm radio} \lesssim \mathbf{2}$ (see Figure 2.5). This is almost certainly significantly less relativistic than the jets produced during transients outbursts of sources such as GRS 1915+105 (Mirabel & Rodríguez 1994; Fender et al. 1999a) and GRO J1655–40 (Hjellming & Rupen 1995; Harmon et al. 1995; see also Fender 2003).
Therefore, if mildly relativistic beaming characterises the low/hard state, a mechanism(s) must exist which both switches the jet off – high/soft state – and produces a faster jet – discrete ejections – above $\sim 10^{-2} L_{\rm Edd}$, where the hard–to–soft state transition occurs.

It is interesting to mention that a few percent of the Eddington rate is also close to the regime at which Ghisellini & Celotti (2001) have identified the transition line between FRI and FR II radio–galaxies, the former class being associated with slower kpc–scale jets than the latter (see Begelman 1982; Bicknell 1984; Laing 1993). This leads to a kind of correspondence between 'extreme sources' like GRS 1915+105, or Cyg X–3, and FRII, characterised by quite high bulk Lorentz factors, while 'canonical' hard state sources would be associated with FR I, with relatively low outflow bulk velocities.

2.7.1 Jet–dominated 'quiescence'

A main task of the models remains that of reproducing the observational behaviour of accreting stellar BHs at a variety of accretion rates. An interesting prediction of this work concerns the relative power of the jet, with respect to the overall accretion power, at low quiescent luminosities.
In this regime, the BH spectral energy distribution appears very similar to that of canonical hard state sources (see Figure 2.7), although the X-ray emission in quiescence is not well reproduced by the standard accretion–corona model, requiring a much lower radiative efficiency.
Narayan et al. (1996, 1997, 2001) showed that an Advection Dominated Accretion Flow (ADAF), in which the energy released by viscous torques is 'stored' into the flow rather than radiated away, can adequately model the available observations at high energies. However, on the other extreme of the spectrum, in

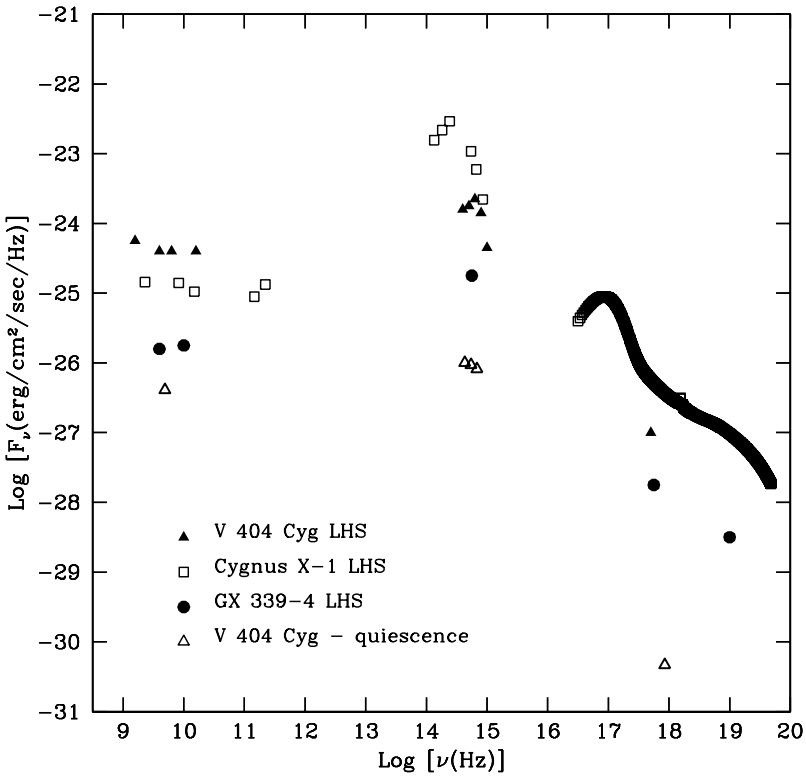

Figure 2.7: Broadband spectra of Cygnus X–1, V 404 Cygni and GX 339–4: for low/hard state (LHS) black holes, not only the behaviour in the $S_{\rm radio}/S_{\rm X}$ plane look very similar, but even the shape of their energy spectrum, from radio wavelengths up to X-rays, suggesting either a common origin or coupling of the basic emission processes.

the radio band, the existence of a jet seriously weakens such a solution, requiring a significantly different physics to model the observed spectrum. Jet–powered radio emission is in fact several orders of magnitude brighter than expected extrapolating ADAF spectra down to radio band; moreover, the standard ADAF picture predicts highly–inverted radio spectra, instead of the observed flat ones. An alternative scenario for low–luminosity stellar black holes has been proposed by Merloni & Fabian (2002). They show that a coronal–outflow dominated accretion disc, in which the fraction of the accretion power released in the corona increases as the accretion rate decreases, would be an ideal site for

jet–launching, both MHD and thermally driven.

Based on the radio:X-ray correlation, the ratio between the observed radio and X-ray luminosities scales as:

$$\frac{L_{\rm radio}}{L_{\rm X}} \propto (L_{\rm X})^{-0.3} \tag{2.8}$$

This already implies that, as the X-ray luminosity decreases, the *radiative* jet power will become more and more important with respect to the X-rays. Moreover, because of the self-absorption effects, it has been shown that there can not be a linear relationship between the radio luminosity, $L_{\rm radio}$, and the *total* jet power, $L_{\rm jet}$, for any optically thick jet model which can explain the flat radio spectrum observed during the hard state. Blandford & Königl (1979), Falcke & Biermann (1996), and Markoff, Falcke & Fender (2001) obtain in fact $L_{\rm radio} \propto (L_{\rm jet})^{1.4}$.
If so, and in general for any relationship of the form:

$$L_{\rm radio} \propto (L_{\rm jet})^{x} \tag{2.9}$$

equation 2.8 implies the following scaling for the fractional jet power:

$$\frac{L_{\rm jet}}{L_{\rm X}} \propto (L_{\rm X})^{(\frac{0.7}{x}-1)} \tag{2.10}$$

Hence, for any $x > 0.7$, there exists an X-ray luminosity below which the jet will be the dominant output channel for the accretion power.
If $x = 1.4$, by re–scaling the numbers to XTE J1118+480 – emitting at $\sim 10^{-3} L_{\rm Edd}$, and whose fractional jet power is at least 20% (Fender et al. 2001) – one obtains that $L_{\rm jet} \gtrsim L_{\rm X}$ for $L_{\rm X} \lesssim 4 \times 10^{-5} L_{\rm Edd}$ (*i.e.* below 0.005 Crab – scaled – see Figure 2.6). Note that observations of GX 339–4 and V 404 Cygni in quiescence already cover this regime, meaning that, if $x = 1.4$, both these sources actually *are* in a jet–dominated state.
This would be a wholly new accretion regime for X-ray binaries, requiring significant modification of existing (e.g. ADAF) models. In addition it would indicate that the overwhelming majority of 'known' stellar–mass black holes, which are currently in quiescence, are in fact feeding back most of their accretion energy into the interstellar medium in the form of the kinetic energy of the jets and are accreting at rather higher levels than derived based only on their X-ray luminosity.
If we do establish that accretion is taking place in quiescence, for instance through the detection of A 0620–00, and is furthermore channelling most of

its power into jet formation, then the arguments for observational evidence for black hole event horizons based upon a comparison of quiescent X-ray luminosities of black hole and neutron star binaries (e.g. Garcia et al. 2001) will need to be re–examined. In fact, assuming that $L_{\rm jet} \propto (L_{\rm X})^{[(0.7/x)]}$ holds for both neutron stars and black holes, then the observed difference in 'radio loudness' between black hole and neutron star binaries (Fender & Kuulkers 2001) might be enough on its own to explain the discrepancy, and it may be that the event horizon plays no part. This is explored further in Fender, Gallo & Jonker (2003; see next Chapter).

2.8 Summary

In this paper we provide observational evidence for a broad empirical relation between radio and X-ray emission in Galactic black hole binaries during their spectrally hard state. The main points established throughout this work can be summarised as follows:

- In low/hard state BHCs the observed radio and X-ray fluxes are correlated over more than three orders of magnitude in accretion rate, with a spread in radio power of about one order of magnitude.

- Even at accretion rates as low as 10^{-5} Eddington a powerful jet appears to be formed; no lower limit to the relation has been found.

- V 404 Cygni is the second source to display $S_{\rm radio} \propto (S_{\rm X})^{\,0.7}$, from quiescence up close to the hard–to–soft state transition.

- Assuming 0.7 as a universal slope for the low/hard state, and under the hypotheses of a) common disc–jet coupling and b) isotropic X-ray emission, the measured spread in radio flux can be interpreted in terms of a distribution in Doppler factors. Monte Carlo simulations show that the observed scatter is consistent with relatively low beaming ($\Gamma_{\rm radio} \lesssim 2$) outflows in the low/hard state, unlike those in transient outbursts.

- When the combination of radio and X-ray beaming is taken into account, the range of possible bulk velocities in the jet significantly broadens, allowing the X-ray emitting material to be relativistic for almost any value of $\Gamma_{\rm radio}$, but implying strong X-ray selection effects. In this case an independent estimation on $\Gamma_{\rm X}$ is needed to limit $\Gamma_{\rm radio}$. Unrelated works (Beloborodov 1999; Maccarone 2003) impose stringent constraints on the

bulk velocity of the X-ray emitting material, leading to the conclusion of relatively low radio beaming ($\Gamma_{\rm radio} \lesssim 2$) in the hard state.

- Close to the hard–to–soft state transition the jet switches off, probably in all sources. The X-ray luminosity at which the radio quenching occurs might positively correlate with the BH mass, being consistent with taking place at a constant fraction of the Eddington rate. It is worth mentioning that a similar fraction of $L_{\rm Edd}$ has been identified as a dividing line between FR I and FR II radio–galaxies, that is between supermassive BHs producing mildly and highly relativistic jets respectively (Ghisellini & Celotti 2001).

- Since the correlation appears to be maintained over many years and for different sources, this leads to the possibility of predicting the level of radio emission from a hard state and/or quiescent BH by measuring its X-ray flux.

- If the radio luminosity scales as the total jet power raised to x, with $x > 0.7$, this implies the existence of an X-ray luminosity below which the most of the accretion power will be channelled into the jet rather than in the X-rays. If $x = 1.4$ (*e.g.* Blandford & Königl 1979, Falcke & Biermann 1996; MFF), then below $L_{\rm X} \simeq 4{\times}10^{-5}\, L_{\rm Edd}$ the jet is expected to dominate.

This work provides evidence for a physical coupling between radio and hard X-ray emitting outflows from accreting stellar BHs. A key, still unresolved issue concerns the modelling of the transition between X-ray states in a self consistent way, which could possibly account for *both* the jet suppression, when the disc dominates, *and* the transition from mildly to highly relativistic jets, as in case of transient outbursts. Including the formation of jets in the overall energetics and dynamics of the accretion process at a variety of X-ray luminosities has undoubtedly become of primary importance to address, especially based on mounting evidence for the jet power to be a significant fraction, if not the dominant output channel, of the total accretion power.

Acknowledgments

The authors wish to thank Sera Markoff, Stephane Corbel, Peter Jonker and Michiel van der Klis, for many useful suggestions and comments on the manuscript. This research has made use of data obtained through the High Energy Astrophysics Science Archive Research Center Online Service, provided

by the NASA/Goddard Space Flight Center. The Ryle telescope is supported by PPARC.

References

Corbel S., Fender R., 2002, ApJ, 573, L35
Corbel S., Nowak M. A., Fender R. P., Tzioumis A. K., Markoff S., 2003, A&A, 400, 1007
Corbel S., Fender R. P., Tzioumis A. K., Nowak M., McIntyre V., Durouchoux P., Sood R., 2000, A&A 359, 251
Corbel S. et al. , 2002, Science, 298, 196
Corbel S. et al. , 2001, ApJ, 554, 43
Cowley A. P., Schmidtke P. C., Hutchings J. B., Crampton D., 2002, ApJ, 123, 1741
Della Valle M., Mirabel I. F., Rodríguez L. F., 1994, A&A, 290, 803
Di Salvo T., Done C., Zycki P. T., Burderi L., Robba N. R., 2001, ApJ, 547, 1024
Done C., 2001, Adv. Space Res., 28, 255
Dubus G., Kim R. S. J., Menou K., Szkody P., Bowen D. V., 2001, ApJ, 553, 307
Ebisawa, K. et al. , 1994, PASJ, 46, 375
Elvis M., Page C. G., Pounds K. A., Ricketts M. J., Turner M. J. L., 1975, Nature, 257, 656
Falcke H., Biermann P. L., 1996, A&A, 308, 321
Fender R. P., 2003, MNRAS, 340, 1353
Fender R. P., 2001a, MNRAS, 322, 31
Fender R. P., 2001b, A&SS, 276, 69
Fender R. P., 2001c, in *'Relativistic flows in Astrophysics'*, Springer Verlag Lecture Notes in Physics, Eds. A.W. Guthmann, M. Georganopoulos, K. Manolakou and A. Marcowith, Lect. Notes Phys. 589, 101
Fender R. P., 2000, in *'Proc. of the Third Microquasar Workshop'*, Eds A. J. Castro–Tirado, J. Greiner and J. M. Paredes, A&SS 276, 69
Fender R. P., Kuulkers E., 2001, MNRAS 324, 923
Fender R. P., Hanson M. M., Pooley G. G., 1999, MNRAS, 308, 473
Fender R. P., Southwell K., Tzioumis A. K., 1998, MNRAS, 298, 692
Fender R. P., Garrington S. T., McKay D. J., Muxlow T. W. B., Pooley G. G., Spencer R. E., Stirling A. M., Waltman E. B., 1999a, MNRAS, 304, 865
Fender R. P. et al. 1999b, ApJ, 519, L165
Galeev A. A., Rosner R., Vaiana G. S., 1979, ApJ, 229, 318

Gallo E., Fender R. P., 2002, MNRAS, 337, 869
Gallo E., Fender R. P., Pooley G. G., 2002, in '*Proc. of the Fourth Microquasars Workshop'*, Eds Ph. Durouchoux, Y. Fuchs, and J. Rodriguez, Center for Space Physics: Kolkata, 201
Geldzahler B. J., 1983, ApJ, 264, L49
Ghisellini G., Celotti A., 2001, A&A, 379, L1
Gierlinski M., Maciolek–Niedzwiecki A., Ebisawa K., 2001, MNRAS, 325, 1253
Greiner J., Dennerl K., Predehl P., 1996, A&A, 314, L21
Haardt F., Maraschi L., 1991, ApJ, 380, L51
Haardt F. et al. , 2001, ApJ, 133, 187
Han X., Hjellming R. M., 1992, ApJ, 400, 304
Hannikainen D. C., Hunstead R. W., Campbell–Wilson D., Sood R. K., 1998, A&A, 337, 460
Harmon B. A., 1995, Nature, 374, 703
Heindl W. A., Prince T. A., Grunsfeld J. M., 1994, ApJ, 430, 829
Hjellming R. M., Rupen M. P., 1995, Nature, 375, 464
Hjellming R. M., Rupen M. P., Mioduszewski A. J., Narayan, R., 2000, The Astronomer's Telegram, 54
Hjellming R. M., Han X., 1995, in *'X-ray binaries'*, Eds. Lewin W. H. G., van Paradijs J., van den Heuvel E. P. J., Cambridge University Press, 308
Homan J., Jonker P. G., van der Klis M., Kuulkers E., 2000, IAU Circ., 7425, 2
Homan J., Wijnands R., van der Klis M., Belloni T., van Paradijs J., Klein–Wolt M., Fender R., Mendez M., 2001, ApJS, 132, 377
Hynes R. I., Steeghs D., Casares J., Charles P. A., O'Brien K., 2003, ApJL, 583, L95
Hynes R. I., Haswell C. A., Chaty S., Shrader C. R., Cui W., 2002, MNRAS, 331, 169
Hynes R. I., Roche P., Charles P. A., Coe M. J., 1999, MNRAS, 305, L49
Keck J. W. et al. , 2001, ApJ, 563, 301
Kitamoto S., Tsunemi H., Pedersen H., Ilovaisky S. A., van der Klis M., 1990, ApJ, 361, 590
Klein–Wolt M., Fender, R. P., Pooley G. G., Belloni T., Migliari S., Morgan E. H., van der Klis M., 2002, MNRAS, 331, 745
Kong A. K. H., McClintock J. E., Garcia M. R., Murray S. S., Barret D., 2002, ApJ, 570, 277
Kotani T. et al. , 2000, ApJ, 543, L133
Kubota A., Makishima K., Ebisawa K., 2001, ApJ, 560, L147
Kuulkers E., Fender R. P., Spencer R. E., Davis R. J., Morison I., 1999,

MNRAS, 306, 919
Laing R. A., 1993, *'Astrophysical Jets'*, ed. D. Burgarella, M. Livio & C. O'Dea Cambridge University Press, 95
Lin D. et al. , 2000, ApJ, 532, 548
Maccarone T. J., 2003, A&A, 409, 697
Maccarone T. J., 2002, MNRAS, 336, 1371
Main D. S., Smith D. M., Heindl W. A. Swank J., Leventhal M., Mirabel I. F., Rodríguez L. F., 1999, ApJ, 525, 901
Markoff S., Falcke H., Fender R.P., 2001, A&AL, 372, L25 (MFF)
Markoff S., Nowak M. A., Corbel S., Fender R., Falcke H., 2003a, A&A, 397, 645
Markoff S., Nowak M., Corbel S., Fender R., Falcke H., 2003b, in Proceedings for *'The Physics of Relativistic Jets in the Chandra and XMM Era'*, Eds. G. Brunetti, D. E. Harris, R. M. Sambruna & G. Setti
Markwardt C. B., Marshall F. E., Swank J. H., 1999, IAU Circ., 7274, 2
Martí J., Mirabel I.F., Duc P.A., Rodríguez L.F., 1997, A&A, 323, 158
Massey P., Johnson K. E., Degioia–Eastwood K., 1995, ApJ, 454, 151
McClintock J. E., Horne K., Remillard R. A., 1995, ApJ, 442, 358
McClintock J. E., et al. , 2001, ApJ, 555, 477
Meier D. L., 2001, ApJ, 548, L9
Merloni A., 2002, in *'Proc. of the Fourth Microquasars Workshop'*, Eds Ph. Durouchoux, Y. Fuchs, and J. Rodriguez, Center for Space Physics: Kolkata, 2105.
Merloni A., Fabian A. C., 2002, MNRAS, 332, 165
Miller J. M., Fox D. W., Di Matteo T., Wijnands R., Belloni T., Pooley D., Kouveliotou C., Lewin W. H. G., 2001, ApJ, 546, 1055
Mirabel I. F., Rodríguez L. F., Nature, 371, 46
Mirabel I. F., Rodríguez L. F., 1999, ARA&A, 37, 409
Mioduszewski A. J., Rupen M. P., Hjellming R. M., Pooley G. G., Waltman E. B., 2001, ApJ, 553, 766
Narayan R., Barret D., McClintock J. E., 1997, ApJ, 482, 448
Narayan R., Garcia M. R., Mcclintock J. E., 2001, in *'Proc. of the Ninth Marcel Grossmann Meeting'*, Eds V. Gurzadyan, R. Jantzen, R. Ruffini, Singapore: World Scientific
Narayan R., McClintock J. E., Yi I., 1996, ApJ, 457, 821
Nowak M. A., 1995, PASP, 107, 1207
Orosz, J. A., 2002, in Proc. of the IAU Symp. 212, Eds K. A. van der Hucht, A. Herraro, & C. Esteban, San Francisco: ASP (astro-ph/0209041)
Orosz J. A., Jain R. K., Bailyn C. D., McClintock J. E., Remillard R. A., 1998,

ApJ, 499, 375
Owen F. N., Balonek T. J., Dickey J., Terzian Y., Gottesman S. T., 1976, ApJ, 203, L15
Parmar A. N., Belloni T., Orlandini M., Dal Fiume D., Orr A., Masetti N., 2000, A&A, 360, L31
Parmar A. N., Stella L., White N. E., 1986, ApJ, 304, 664
Pooley G. G., Fender R., Brocksopp C., 1999, MNRAS, 302, L1
Pooley G. G., Fender R., 1997, MNRAS, 292, 925
Poutanen J., 1998, in *'Theory of Black Hole Accretion Disks'*, Camridge University Press, 100
Poutanen J., Svensson R., 1996, ApJ, 470, 249
Predehl P., Burwitz V., Paerels F., Trmper J., 2000, A&A, 357, 25
Robinson E. L., Ivans I. I., Welsh W. F., 2002, ApJ, 565, 1169
Rutledge R. E., Bildsten L., Brown E. F., Pavlov G. G., Zavlin V. E., 1999, ApJ, 514, 945
Sánchez–Ferández C. et al. , 1999, A&A, 348, L9
Schulz N. S., Cui W., Canizares C. R., Marshall H. L., Lee J. C., Miller J. M., Lewin W. H. G., 2002, ApJ, 565, 1141
Shahbaz T., Naylor T., Charles P. A., 1994, MNRAS, 268, 756
Shakura N. I., Sunyaev R. A., 1973, A&A 24, 337
Shapiro S. L., Lightman A. P., Eardley D. M., 1976, ApJ, 204, 187
Shrader C. R., Wagner R. M., Charles P. A., Harlaftis E. T., Naylor T., 1997, ApJ, 487, 858
Sobczak G. J., McClintock J. E., Remillard R. A., Levine A. M., Morgan E. H., Bailyn C. D., Orosz J., 1999, ApJ, 517, L121
Sood R., Campbell–Wilson D., 1994, IAU Circ., 6006, 1
Stirling A. M., Spencer R. E., de la Force C. J., Garrett M. A., Fender R. P., Ogley R. N., 2001, MNRAS, 327, 1273
Sunyaev R. A., Titarchk L. G., 1980, A&A, 86, 121
Sunyaev R. A. et al. , 1991, ApJ, 383, L49
Tanaka Y., 1993, IAU Circ., 5877, 1
Terasawa N., Nakamura H., 1995, A&A, 294, 443
Tomsick J. A., Kaaret P., 2000, ApJ, 537, 448
Ueda Y., Inoue H., Tanaka Y., Ebisawa K., Nagase F., Kotani T., Gehrels N., 1998, ApJ, 492, 782; erratum ApJ, 500, 1069
van Kerkwijk M. H. et al. , 1992, Nature, 355, 703
Wagner R. M., Starrfield S. G., Hjellming R. M., Howell S. B., Kreidl T. J., 1994, ApJ 429, L25
Wilms J., Nowak M. A., Pottschmidt K., Heindl W. A., Dove J. B., Begelman

M. C., 2001, MNRAS, 320, 327
Zdziarski A. A., Gilfanov M., Lubinski P., Revnivtsev M., 2003, MNRAS, 342, 372
Zdziarski A. A., Poutanen J., Mikolajewska J., Gierlinski M., Ebisawa K., Johnson W. N., 1998, MNRAS, 301, 435
Zycki P. T., Done C., Smith D. A., 1999, MNRAS, 305, 231